NCI : looking at solute/solvent interactions

Robin Chaudret, C. Narth, Raphaël Lugo, Pascal Mougin, Jean-Charles de Hemptinne, Hervé Toulhoat, J. Contreras-García

NCI: looking at solute/solvent interactions

R. Chaudret[1,*], C. Narth[3], R. Lugo[1], P. Mougin[1,2], J.-C. de Hemptinne[1], H. Toulhoat[1], J. Contreras-García[3,*]

[1] IFPEN, 1-4 Avenue du Bois Préau, 92852 Rueil-Malmaison, France
[2] Sorbonne Université, CNRS, Laboratoire de Réactivité de Surface, F. 75005 Paris, France
[3] Sorbonne Université, CNRS, Laboratoire de Chimie Théorique, LCT, F. 75005 Paris, France

Abstract

Understanding solvation interactions is a key problem for many industrial fields: from pharmaceutical to material sciences. From a quantum mechanical viewpoint, two main difficulties arise: firstly, solvation takes place through weak interactions (hydrogen bonds, van der Waals interactions), which are inherently difficult to describe. Secondly, solvation properties are dynamic in nature, which means a proper statistical averaging is required to reproduce experimental properties. In this contribution, we dwell on the analysis of solute-solvent interactions by means of the averaged-NCI index, derived from an MD averaged picture of the electron density in the system. Firstly, we show how the approach enables to distinguish static vs labile and strong vs weak hydrogen bonds. Then, by means of this approach we are able to characterize the fact that the strength of hydrogen bonds with water solvent remains similar upon branching for aliphatic alcohols. On the contrary large differences have been observed between aliphatic alcohols and phenol derivatives. This statistical analysis of interactions is expected to be useful in the derivation of microscopic parameters for solute/solvent interactions.

Introduction

Understanding solvation interactions is a key problem for many industrial fields: from pharmaceutical to material sciences. Within a biological context, solution of drugs is crucial for their transport in the body and hence their interaction with the target (1). Similarly, catalysts in complex media need to favorably solvate in the right phase or else they cannot be active even if their theoretical efficiency is high (2). All these solvation processes might involve complex physicochemical processes, such as van der Waals and other inherently many-body interactions

(3; 4; 5; 6; 7; 8; 9; 10). In order to predict and improve macroscopic solvation interaction, several tools have been designed such as the QSPR approaches and the SAFT equations (11; 12). However, such approaches usually require experimental data that is expensive to obtain or even not accessible. Alternatively, it is possible to connect the parameters in these approaches to solute/solvent interactions from a microscopic point of view. Hence, it is interesting to develop approaches that recover a time average of this microscopic information. However, this requires the interaction analysis to be embedded through statistical analysis.

Averaged NCI (*aka* aNCI) falls within that challenging context, enabling micro- and macroscopic insights thanks to its statistical averaging. The original NCI approach is based on the electron density, ρ, and was developed as a static approach to non-covalent interactions by Jonhson et al. in 2010 (13). It allows the visualization of non-covalent interactions within any type of chemical system, such as organic, inorganic, enzymatic, reactive, etc. (14; 15; 16; 17; 18; 19). More recently, Wu et al. proposed a new topological approach based on NCI that allows the visualization of the averaged non-covalent interactions (aNCI) from molecular dynamics (20), leading to the required statistical information needed to study solvation. In this paper we apply the aNCI approach to investigate the interaction between several different alcohol molecules and solvent in order to analyze how substitution and functionalization are revealed in the dynamic solute/solvent interactions. With this aim in mind, several aliphatic chains are tested as well as various substituted phenols. Finally, the influence of the solvent on the microscopic interactions structure and on the relative stability of different species is investigated.

Method

Electronic structure

The solute structures were minimized at the quantum level using Gaussian09 software 6-31++G** basis set and the B3LYP functional (21; 22; 23; 24). Once optimized, structures were kept frozen during the molecular dynamics (MD) simulations to firstly relax the solvent and then let it evolve around the solute molecule.

The system was set up so that a single solute molecule was placed in the center of a cubic box of equilibrated solvent molecules within a distance from its boundaries of at least 15Å. The systems were first minimized using 5000 steps of steepest descent and conjugated gradient, then warmed from 50 to 300 K with a pressure of 1 atm during 150 ps in the NPT ensemble to reach density solvent convergence. Finally, 1 ns of MD in the NVT ensemble was performed

(T=300K) saving configuration snapshots every 1 ps. With this approach, we obtained 1000 configurations to represent the MD space phase exploration and to analyze weak interactions.

Casting weak interactions: averaged NCI

The Reduced Density Gradient, RDG or s(ρ) (25) was applied to each of the snapshots. This index has been shown to provide useful representation of non-covalent interactions such as steric clashes, hydrogen bonds or van der Waals interactions (14). This is based on the fact that s(ρ) assumes values approaching zero for regions of both covalent bonding and non-covalent interactions. These low s(ρ) areas are traced back to molecular space giving rise to isosurfaces that enable to visualize the weak interactions of the system. The value of the density in these regions can be used to semi-quantitatively estimate the relative strength of the interactions, whereas the sign of the second eigenvalue of the density hessian matrix, λ_2, is used to differentiate between attractive and repulsive interactions (see refs (13; 14; 25) for more details). Therefore, by coloring the low RDG area in the molecular space as a function of $sign(\lambda_2)*\rho$, it is possible to visualize the weak interactions and their strength. In this paper, we will use the following color code:

- Blue for the highly attractive weak interactions (such as hydrogen bonds), $sign(\lambda_2)*\rho < 0$.
- Green for the extremely weak interactions (such as van der Waals), $sign(\lambda_2)*\rho \approx 0$.
- Red for repulsive interactions (such as steric clashes), $sign(\lambda_2)*\rho > 0$.

Results for methanol and six water molecules are shown in Figure 1a. The interaction between the methanol alcohol functional group and the surrounding molecules at 1.8-2.0 Å showcase typical NCI images of hydrogen bonds: blue circular pellets apppear. The three water molecules interacting with the CH_3 moiety illustrate how NCI renders weaker van der Waals adirectional interactions. In this case, the surfaces are thin green films. Whereas the strength of the interaction is usually casted by distances, this approach enables to estimate it from the electron density. Since this density is used to color the isosurfaces, the strength of the interaction is included in a very visual manner: blue for strong interactions and green for weak ones.

a) b) c) d)

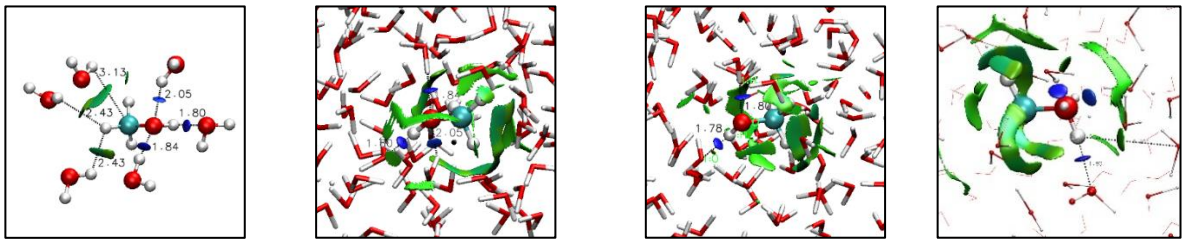

Figure 1: NCI analysis of methanol and water molecules. a) Methanol and 6 isolated water molecules b) NCI analysis of the same disposition as in a) but with the full water environment. c) another snapshot where there is only one hydrogen bond through the O atom d) 2nd coordination water in snapshot b) highlighted.

To deal with large systems, a promolecular approach has been introduced. The density of the total molecule is approximated as the sum of the atomic densities already parameterized and stored within the program. From a numerical point of view, this approach is much faster than using relaxed densities while keeping qualitatively good agreement with the full QM approach. Hence, it opens new perspectives of ambitious applications in the supramolecular framework. As an example, promolecular approaches have allowed dealing with larger systems such as protein conformations or protein/ligand interactions. The approach has now been widely used to study interactions within metallic systems, organic, inorganic and enzymatic reactivity, solid and surface systems (14; 17). It also enables analyzing static interactions of solute molecules within a solvent. Figures 1b and 1c exemplify how the solute interactions with a full water environment differ from some isolated molecules (Figure 1a). Larger van der Waals interactions appear due to the full surrounding water environment. Nevertheless, the analysis of different snapshots enables to see how the interactions might change during a MD trajectory: both in Figures 1b and 1c the hydrogen bond through the H is present, but the hydrogen bonds through the oxygen lone pairs differs. Whereas there are two hydrogen bonds in the snapshot from Figure 1b, there is only one in Figure 1c.

This reflects the necessity for an averaged approach to accurately represent the interactions within fluctuating systems (20). The NCI approach is based on the study of the interactions within one structure that is supposed to be representative of the state of the system. However in dynamic systems (such as solute/solvent ones), it is not one single structure but an ensemble of structures that will be characteristic of the system. Therefore, it is not one interaction but an ensemble of interactions that one should take into account in order to understand solute/solvent problems. With this idea in mind, Wu et al. modified the NCI index into an average Non

Covalent Interaction (aNCI) index looking at the gradient of the averaged density (<ρ>) as a function of the averaged density (20).

The analysis starts by sampling the conformations of a large system: solvent (large cubic box) or protein and solvent describing a realistic chemical environment around the target molecule (e.g. the solute or the ligand). This can be done at any level of theory and statistical approaches (QM/MM, MM, dynamic or Monte-Carlo). For the average to be meaningful, the target molecule has to be rigid along the simulation, ensuring that the solute/ligand accessibility by solvent molecules is representative. This approach can be repeated in order to take various solute orientations into account.

As an example, Figure 2a shows the aNCI picture for the MD trajectory of methanol in water: the average of NCI interactions over the full trajectory. We can see how the hydrogen mediated hydrogen bond (HBH), present in most trajectories as we saw in Figs 1b-c, leads to a blue surface very similar to the individual snapshots. Instead, in the case of the oxygen mediated hydrogen bond, the greater mobility leads to a continuous surface connecting both lone pairs, with bluer surfaces at the lone pairs (HBO1, HBO2) -which are less blue than HBH-, but a non-negligible probability of interaction with the oxygen through the space in between the HBO1 and HBO2. As for the van der Waals interactions, that are more delocalized, bigger surfaces appear all around the molecule. These surfaces are also further away, since the typical van der Waals distance of the solvent water is larger than the hydrogen bonded one. Note that this image can be related to the RDF found for the same system (Figure 2b): the hydrogen bond leads to a sharp peak, whereas the vdW interactions lead to a wider and further away peak. When Fig. 2a and 2b are compared, we can see that the typical aNCI image typically recovers the information in the well-formed peaks in the RDF: the one due to hydrogen bonds at ca. 2Å in blue, and closer to the methanol molecule; and the one due to van der Waals interactions at ca. 3.8Å in green, and further away from the reference molecule. This is the case for C, but also for the alcohol atoms (as illustrated in Fig 1d and the wide green second peak in Fig. 2b).

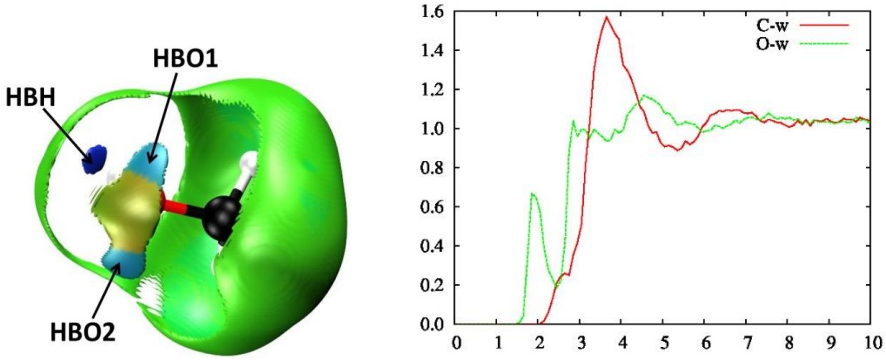

Figure 2: a) aNCI analysis of the methanol/water solute/solvent interactions and label of the different interactions: HBH for the hydrogen bond through the hydrogen and HBO1, HBO2 for the hydrogen bonds through the oxygen lone pairs. b) RDF for MeOH carbon (C-water) and oxygen atoms (Oxygen-water).

All in all, the aNCI approach assembles in a visual manner information from directional interactions (first coordination spheres), identifying which ones are stronger and localized, or weaker and delocalized. The number of blue zones provides information on the number of hydrogen bonds, and the region in between then can inform us on their nature, i.e. dynamic vs static hydrogen bonds. The latter information is recovered thanks to the averaging over the MD trajectory of the electron density, which is mathematically acceptable due to the definition of ensemble densities. This approach would be more difficult to implement for example if graphs were used, due to the disconnected nature of graphs over the trajectory. Since the approach is based on the electron density, it is applicable to any interaction type, irrespective of their nature. Nonetheless, no partition is associated, so only the final strength can be assessed, not the origin (charge transfer, polarization) of the interaction.

In the current study, the aNCI analysis was performed using a modified version of NCIplot (14) and 800 configurations. For the linear and the branched alcohol in water, the RDG cutoff was set to 0.2 and $\lambda_2*\rho$ varied between -0.03 a.u. (atomic units) and 0.03 a.u. For phenol derivatives in water (where van der Waals interactions are more important), the RDG cutoff was set to 0.3 and $\lambda_2*\rho$ varied between -0.02 a.u. and 0.02 a.u. For the rest of the molecules, the cutoff will be specified along with their analysis.

Results and discussion:

1.Variations in the solute

a) Aliphatic alcohols

On top of the methanol example above, we have first analyzed the interactions in several linear and branched alcohol molecules (ethanol, iso-propanol and tert-propanol) in water solvent. Alike the methanol example, these alcohols show one strong anisotropic hydrogen bond between the alcohol proton and the solvent (HBH interaction) and two localized interactions at the position of the alcohol oxygen lone pairs (HBO1 and HBO2 interactions), see Figures 2 and 3.

The HBH interaction is stronger and more localized than the HBO ones (ρ(HBH) ≈ 0.030 a.u. and ρ(HBO) ≈ 0.017 a.u., respectively). Both interaction types remain rather constant along the alcohol series (see Figure 3 and Table 1) with the exception of the tert-butanol. For tert-butanol, the HBO interactions are stronger at the expense of the HBH interaction, which becomes weaker. The differences in tert-butanol are due to the absence of α-H with respect to the oxygen as well as the smaller accessibility due to the increased steric hindrance due to the conformation. This hindrance leads to all hydrogen bonds being localized (the connection between the oxygen lone pairs is lots). In all cases, the CH_3 groups interact with the water solvent through delocalized van der Waals interactions.

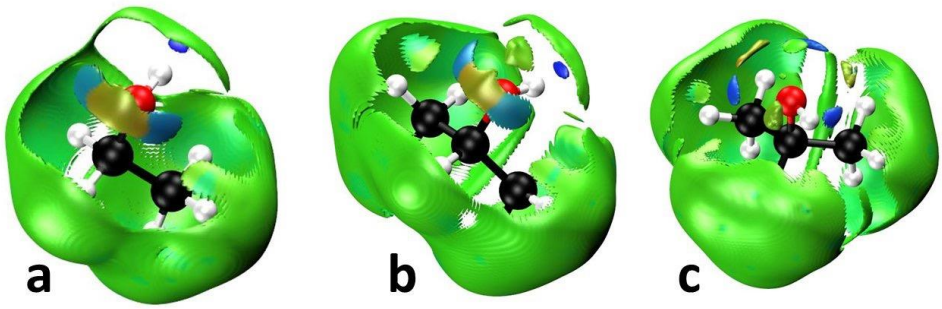

Figure 3: aNCI analysis of (a) ethanol/water, (b) iso-propanol/water and (c) tert-butanol/water solute/solvent interactions.

Molecule	ρ_{cp}(HBH)	ρ_{cp}(HBO1)	ρ_{cp}(HBO2)
Methanol	0.028	0.017	0.017
Ethanol	0.030	0.019	0.016
n-Propanol	0.029	0.018	0.015
Iso-propanol	0.028	0.018	0.017
Tert-butanol	0.025	0.024	0.024

Table 1: Value of the density at the critical point (a.u.) between methanol, ethanol, propanol, iso-propanol and tert-butanol molecules and water solvent. Note that values are obtained using classical simulations. The values are computed on frozen molecules and averaged over solvent conformation. The values reported are from the averaged density at the critical point.

Since this analysis is done at fixed alcohol geometry, we have also investigated the influence of the alcohol structure on the value of the HBH and HBO interactions. We performed

a 2D scan over Φ and Ψ dihedrals of butan-2-ol molecule defined in Scheme 1. All the results are summarized in supplementary information movies **M1**, **M2**, **M3** and **M4**. They show that for the most stable conformations, the HBH and HBO interactions remain rather similar, ranking between 0.015 a.u. and 0.020 a.u. for the HBO interactions and between 0.030 a.u. and 0.032 a.u. for the HBH ones. However, at some specific angles corresponding to bigger steric repulsions between the methyl group and the alcohol proton, stronger differences can appear. In these cases, the HBO interactions with the lone pairs can drop to 0.012 a.u.

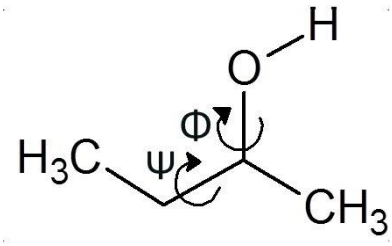

Scheme 1: Scheme of the butan-2-ol and label of the dihedral involved in the 2D scan.

b) Phenols

We can expect the van der Waals interactions to be favored in the case of benzene rings. This also leads to changes in the alcohol properties (reduced pKa, lone pair delocalized in π-system, etc). Hence, we have analyzed several phenol derivatives (shown in Figure 4).

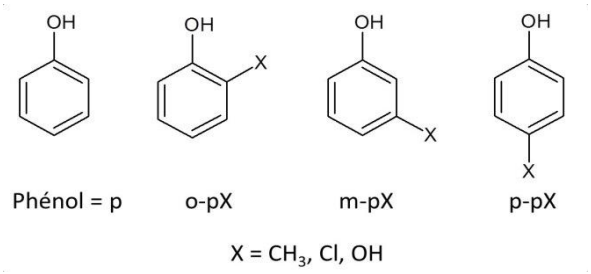

Figure 4: Scheme of the different phenol derivatives studied

As expected, the phenol derivatives interactions (Figures 5 and S1) differ notoriously from the aliphatic alcohols. Whereas the shape of HBH interaction is not much affected, important differences emerge for the HBO interactions. Instead of the two HBO interactions found in aliphatic alcohols, only one hydrogen bond through the lone pair is observed for the phenol derivatives. This can be attributed to the delocalization of one of the oxygen lone pairs into the phenyl π-system, thus participating in the OH···π interactions between the phenyl ring and the surrounding water solvent molecules.

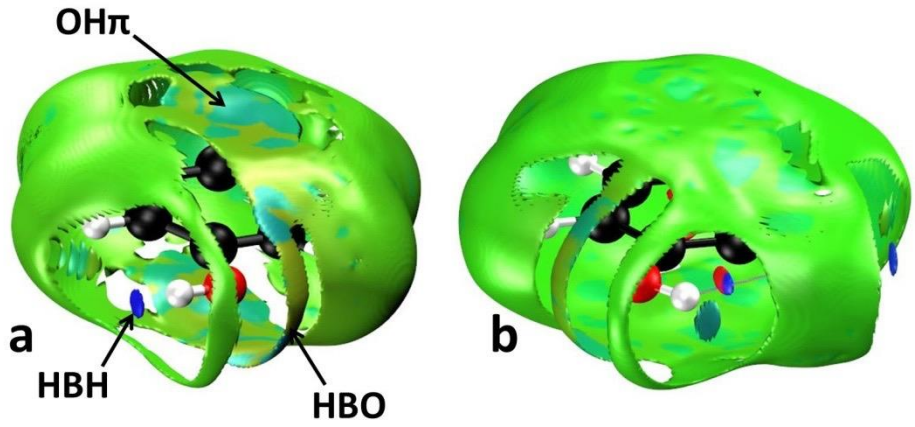

Figure 5: aNCI analysis of phenol/water (a) and catechol(o-pOH)/water (b) solute/solvent interactions. The name of the interactions is labeled for phenol (a). For catechol (b), the NCI isosurface of the intramolecular interaction is also shown.

Various phenol substituents were chosen to analyze different electronic effects on the π system: mesomer donor (OH), inductor donor (CH_3) and inductor acceptor (Cl) (Figure 4). Table 2 shows the evolution of the HBH, HBO and OH-π interactions as the substituent and its localization (ortho, meta, para) are modified. For all these simulations no major differences are found for the different molecules except for the o-pOH and o-pCl ones. In these two cases, an intramolecular hydrogen bond between the -OH group of the phenol and the substituent (-OH or –Cl) is created that modifies the properties of the solute/solvent interactions. In the case of o-pCl the –OH hydrogen interacts with the Cl atom and therefore the strength of its HBH interaction decreases (dropping from ca. 0.026 a.u. to 0.013 a.u.). For o-pOH, an intramolecular hydrogen bond is created (Figure 5b). The oxygen lone pair involved in the intramolecular interaction is therefore not available to create intermolecular interactions with the solvent.

Molécule	**HBH**	**HBO**	**OH-π**
Phenol	0.024	0.011	0.008
o-pOH	0.033	0.000	0.007
m-pOH	0.032	0.015	0.012
p-pOH	0.033	0.013	0.010

o-pCl	0.016	0.012	0.006
m-pCl	0.032	0.011	0.006
p-pCl	0.030	0.012	0.005
o-pCH$_3$	0.030	0.016	0.009
m-pCH$_3$	0.032	0.014	0.011
p-pCH$_3$	0.028	0.012	0.0094

Table 2: Value of the density at the critical point of interaction (a.u.) for the phenol derivatives (Figure 4) and water solvent.

Neutral and charged amines

Methylamine and methylamonium ions were also studied. Figure 6 shows a representative example of neutral and charged amines. All data are collected in Table 3. Just like in the case of the alcohols, we have found hydrogen bonds between the solvent and hydrogen atoms (HBH) and between the solvent the lone pair of the nitrogen atom (HBN). HBN interactions show greater densities than HBO ones in alcohols. Ammonium salts show the strongest HBH interacting densities. Moreover, the trends are inverted from the alcohols to the amines: whereas the HBH is the strongest one in alcohols, and the most localized (forming a clear disk), in amines the strongest and most localized hydrogen bond is through the nitrogen lone pair (HBN). This correlates with the stronger electronegativity of the oxygen atom, which favors OH-N interactions rather than NH-O. This leads to highly delocalized NH-O interactions subsumed within the vdW envelop.

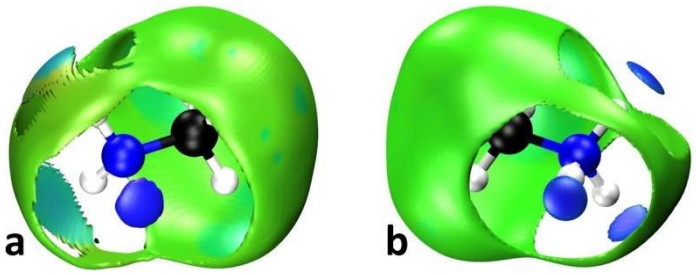

Figure 6: aNCI analysis of methylamine/water (a) and methylamonium/water (b) solute/solvent interactions.

Molecule	HBH1	HBH2	HBH3	HBN
Methylamine	0.013	0.010	X	0.027
Ethylamine	0.009	0.009	X	0.027
n-propylamine	0.010	0.010	X	0.027
Iso-propylamine	0.009	0.009	X	0.027
Methylamonium	0.029	0.029	0.027	X
Ethylamonium	0.030	0.030	0.028	X
Iso-propylamonium	0.032	0.031	0.029	X

Table 3: Value of the density at the critical point of interaction (a.u.) for interactions between various amine molecules or ammonium cation and water solvent.

Overall, we have shown that the aNCI analysis is able to model the interactions in a diverse set of solutes immersed in water (hydrogen bonds, OH-π or van der Waals interactions). It is also able to reproduce the variations of electrophilicity or nucleophilicity between the different groups. Additionally, it allows to correctly reproduce the expected hydrogen bonds as well as the weaker interactions such as the OH-π interactions in phenol.

2. Variations in the solvent

2.1. ethanol and phenol

In this section, we investigate the variation of the solute/solvent interactions upon solvent modification. We first looked at the difference of interactions between ethanol in water and ethanol in ethanol. The results are presented in Figure 7. In both cases a major difference arises for the HBO interactions: in both cases only one HBO remains. Hence, instead of obtaining the delocalized interaction with the two lone pairs, we obtain a unique large blue surface. This is simply due to the hydrogen bond donating possibilities of the solvent. Whereas water solvent has two H-bond donors, ethanol only has one hydrogen bond donor (in all cases we have two H-bond acceptors). Hence, only one HBO is present (the size of ethanol hampers the lone pairs of two different ethanol molecules approaching). In this case, the interaction through the lone pair is expected to be very dynamic, as seen from the extended blue color all along the large NCI surface.

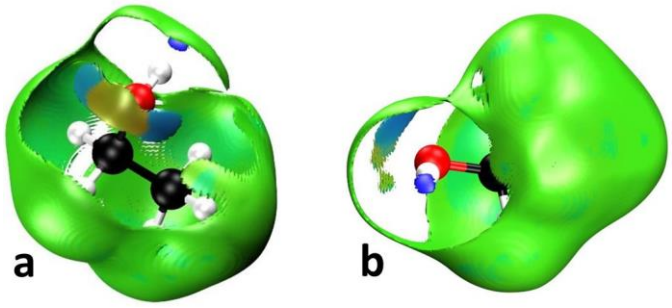

Figure 7: aNCI analysis of ethanol/water (a) and ethanol/ethanol (b) solute/solvent interactions.

Similar results are obtained in the case of the OH-O hydrogen bond in phenol solvated by phenol (Figure 8). However, in this case, important differences appear for the O···π interaction. The use of phenol as solvent induces the disappearance of the O···π interaction as well as a better localization of the hydrogen bonds. This reveals that liquid phenol prefers a stacked layered orientation, where the hydrogen bonds are favored over O···π interactions (which would require a T-shape orientation).

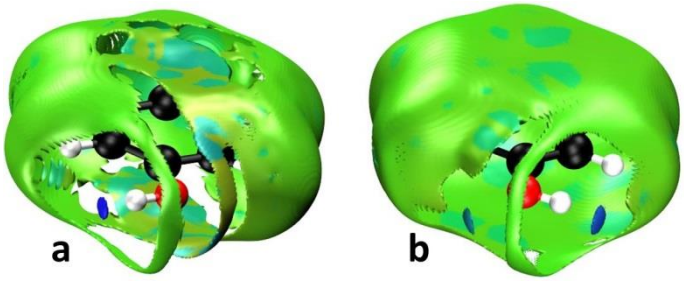

Figure 8: aNCI analysis of phenol/water (a) and phenol/phenol (b) solute/solvent interactions.

2.2. 1,3-dicarbonyl

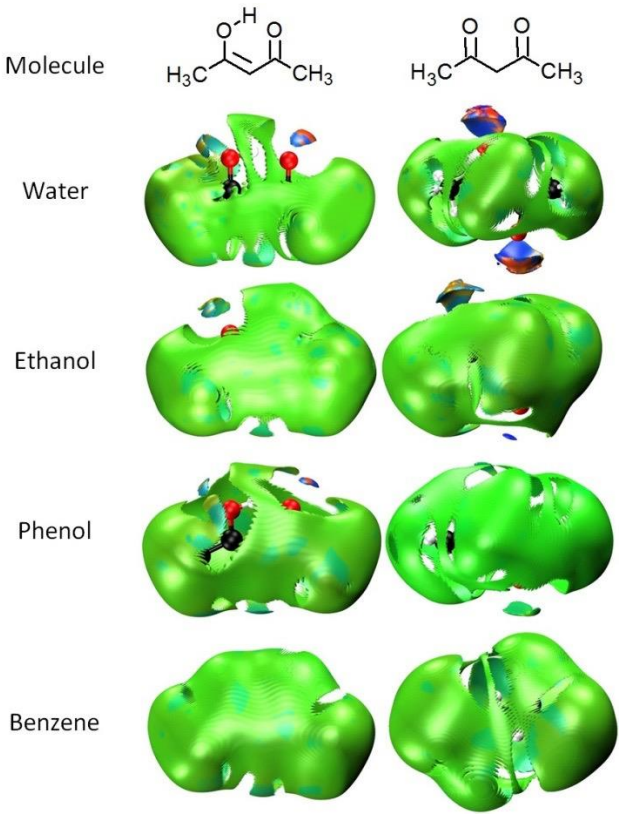

Figure 9: aNCI analysis of the keto and enol forms of 1,3-dicarbonyl compound in water, ethanol, phenol and benzene solvents. Keto form on the right, and enol on the left.

We have performed an analysis of a carbonyl compound in order to analyze the ability of aNCI to explain the stability of different tautomers. The aNCI analysis of the keto and enol forms of the 1,3-dicarbonyl compound have been studied in water, ethanol, phenol and benzene solvents (see Figure 9).

The interaction between the oxygen of a C=O bond and the water the acetaldehyde molecule is stronger than that of the OH, to the point that two clear interactions appear between the lone pairs in C=O and only a general delocalized interaction is present for the OH. When we move to the ketone this effect is boosted further, in agreement with the respective nucleophilicity and basicity.

As we move down the solvent list, we see that the less protic the solvent, the stronger the van der Waals interactions (and the weaker the interactions with the oxygen atoms). This simple picture enables to understand the enol/keto ratio in the different solvents (Table 4). In the gas phase the enol form is more stabilized due to the very strong intramolecular hydrogen bond, this ratio is conserved in benzene because the van der Waals interactions are quite similar in

both forms. On the contrary the ratio tends to decrease strongly when using ethanol and water solvent. The aNCI analysis clearly shows the oxygens atoms of the keto form has a stronger interaction with these solvents than the oxygens of the enol form, where the intramolecular hydrogen bond competes with intermolecular interactions.

Solvent	K_T
Gas phase	11.7
Benzene	14.7
Ethanol	5.8
Water	0.23

Table 4: Evolution of K_T = [enol form] / [keto form] of 1,3-dicarbonyl compound in gas phase, water, ethanol and benzene solvents.

Conclusion

The aNCI index (20), which allows visualization of averaged weak interactions over a trajectory has been applied to understand solute-solvent interactions in some typical functional groups and solvents. Such approach allows for example to quantify the average strength and number of the solute/solvent hydrogen bonds without using triggering criteria (distance or angle cutoff for example): it suffices to identify blue surfaces on the aNCI plot. Moreover, the static or dynamic nature of this hydrogen bonds is also easily identified in terms of the shape of the surface: departing from the disk shape as the interaction becomes more dynamic. The distance at which the surfaces appear also provide information about the sphere of coordination we are looking at, highlighting that the concept first and second sphere is only local: the van der Waals RDF peak in methanol illustrates how these interaction can actually belong to the second sphere (around the alcohol group) but also to the first coordination sphere (around the CH_3 group).

In order to exploit this information, we have analyzed a set of aliphatic alcohols in water and shown that the strength of the hydrogen bonds remains similar upon branching: the hydrogen mediated bond is stronger and more localized, whereas the oxygen mediated hydrogen bond is weaker and more dynamic. The one exception is tert-butanol, where the hindrance limits this dynamicity. When phenol derivatives are analyzed, the number of available lone pairs

diminished, due to its localization within the ring. Instead, this favors the interaction of water with the π ring. The introduction of substituents leading to intramolecular interactions further diminishes the available lone pairs, which should have a direct effect on their solubility in water.

Several aliphatic amine molecules and ammonium cations were also studied. For these systems, the strength of the hydrogen bonds on the hydrogen (HBH) decreases whereas it increases for the hydrogen bonds on the nitrogen (HBN). These findings follow the evolution of the electrophilicity of the hydrogen and nucleophilicity of the oxygen and nitrogen atoms, favoring the OH-N interactions over the NH-O ones. This provides a clear trend for the organization of liquids containing these functional groups.

Finally, we showed that the nature of the aNCI approach was able to reproduce the modifications of solute/solvent interactions when changing the solvent. Interestingly, the preference for stacking interactions rather than OH-π ones appeared very visually for liquid phenol as opposed to the previous analysis of phenol in water. Finally, we were able to explain the evolution of the keto-enolic equilibrium of 1,3-dicarbonyl compound within different solvents due to the competition of intra and intermolecular hydrogen bonds in the enol tautomer.

Overall, we have carried a cross analysis of solutes in different solvents as well as of solvent conformation with the aNCI approach, showing that it provides a visual approach to strength, dynamicity, distances and local information in a unique and intuitive picture.

Supporting Information

Figure S1 and movies M1-M4 are available online and free of charge.

Acknowledgments

We thank E. Rezabal for counseling with the calculations.

References

1. *Drug-like properties and the causes of poor solubility and poor permeability. Journal of pharmacological and toxicological methods.* **Lipinski, C. A.** 2000, Vol. 44, pp. 235-249.
2. **Purbrick, M. D.** *Phase-transfer catalysis: fundamentals, applications and industrial perspectives. Charles M. Starks, Charles L. Liotta and Marc Halpern.* London : Chapman & Hall, 1995. ISBN 0-412-04071-9.
3. **Reichardt, C., & Welton, T.** *Solvents and solvent effects in organic chemistry.* s.l. : John Wiley & Sons, 2011.

4. *Role of water in super growth of single-walled carbon nanotube carpets.* **Amama, P. B., Pint, C. L., McJilton, L., Kim, S. M., Stach, E. A., Murray, P. T., ... & Maruyama, B.** 2008, Nano letters, Vol. 9, pp. 44-49.
5. *Enzymatic catalysis in monophasic organic solvents. Enzyme and Microbial Technology.* **Dordick, J. S.** 1989, Vol. 11, pp. 194-211.
6. *How solvent controls electronic energy transfer and light harvesting.* **Scholes, G. D., Curutchet, C., Mennucci, B., Cammi, R., & Tomasi, J.** 2007, The Journal of Physical Chemistry B, Vol. 111, pp. 6978-6982.
7. *The role of water in gaseous biocatalysis.* **Robert, H. R., Parvaresh, F., & Legoy, M. D.** 2014, Progress in Biotechnology; Biocatalysis in Non-Conventional Media, pp. 85-93.
8. *Improving enzymes by using them in organic solvents.* **Klibanov, A. M.** 2001, Nature, Vol. 409, pp. 241-246.
9. *Wet and dry interfaces: the role of solvent in protein–protein and protein–DNA recognition.* **Janin, J.** 1999, Structure, Vol. 7, pp. R277-R279.
10. *Role of water in the enzymatic catalysis: study of ATP+ AMP→ 2ADP conversion by adenylate kinase.* **Adkar, B. V., Jana, B., & Bagchi, B.** 2010, The Journal of Physical Chemistry A, Vol. 115, pp. 3691-3697.
11. *The importance of being earnest: validation is the absolute essential for successful application and interpretation of QSPR models. QSAR & Combinatorial Science.* **Tropsha, A., Gramatica, P., & Gombar, V. K.** 2003, Vol. 22, pp. 69-77.
12. *Statistical associating fluid theory: a successful model for the calculation of thermodynamic and phase equilibrium properties of complex fluid mixtures. Industrial & engineering chemistry research.* **Economou, I. G.** 2002, Vol. 41, pp. 953-962.
13. *Revealing noncovalent interactions.* **Johnson, E. R., Keinan, S., Mori-Sanchez, P., Contreras-Garcia, J., Cohen, A. J., & Yang, W.** 2010, Journal of the American Chemical Society, Vol. 132, pp. 6498-6506.
14. *NCIPLOT: a program for plotting noncovalent interaction regions. Journal of chemical theory and computation.* **Contreras-García, J., Johnson, E. R., Keinan, S., Chaudret, R., Piquemal, J. P., Beratan, D. N., & Yang, W.** 2011, Vol. 7, pp. 625-632.
15. *Revealing non-covalent interactions in solids: NCI plots revisited.* **Otero-de-la-Roza, A., Johnson, E. R., & Contreras-García, J.** 2012, Physical Chemistry Chemical Physics, Vol. 14, pp. 12165-12172.
16. *Coupling quantum interpretative techniques: another look at chemical mechanisms in organic reactions. Journal of chemical theory and computation.* **Gillet, N., Chaudret, R., Contreras-García, J., Yang, W., Silvi, B., & Piquemal, J. P.** 2012, Vol. 8, pp. 3993-3997.
17. **Narth, C., Maroun, Z., Boto, R. A., Chaudret, R., Bonnet, M. L., Piquemal, J. P., & Contreras-García, J.** *In Applications of Topological Methods in Molecular Chemistry. A complete NCI perspective: from new bonds to reactivity.* s.l. : Springer, 2016. pp. 491-527.
18. *Guest–host interactions in gas clathrate hydrates under pressure.* **Izquierdo-Ruiz, F., Otero-de-la-Roza, A., Contreras-García, J., Menéndez, J. M., Prieto-Ballesteros, O., & Recio, J. M.** 2015, High Pressure Research, Vol. 35, pp. 49-56.
19. *Toward a deeper understanding of enzyme reactions using the coupled ELF/NCI analysis: application to dna repair enzymes.* **Fang, D., Chaudret, R., Piquemal, J. P., & Cisneros, G. A.** 2013, Journal of Chemical Theory and Computation, Vol. 9, pp. 2156-2160.
20. *Noncovalent interaction analysis in fluctuating environments.* **Wu, P., Chaudret, R., Hu, X., & Yang, W.** 2013, Journal of chemical theory and computation, Vol. 9, pp. 2226-2234.
21. **Frisch, M. J., et al.** *Gaussian 09, Revision E.01.* Wallingford CT : D. J. Gaussian, Inc., 2009.
22. *The influence of polarization functions on molecular orbital hydrogenation energies.* **Hariharan, P. C., & Pople, J. A.** 1973, Theoretica chimica acta, Vol. 28, pp. 213-222.

23. *Density-functional thermochemistry. III. The role of exact exchange.* **Becke, A. D.** 1993, The Journal of chemical physics, Vol. 98, pp. 5648-5652.
24. *Development of the Colle-Salvetti correlation-energy formula into a functional of the electron density.* **Lee, C., Yang, W., & Parr, R. G.** 1988, Physical review B, Vol. 37, p. 785.
25. *Interpretation of the reduced density gradient.* **Boto, R. A., Contreras-García, J., Tierny, J., & Piquemal, J. P.** 2016, Molecular Physics, Vol. 114, pp. 1406-1414.
26. **Plimpton, S., Crozier, P., & Thompson, A.** *LAMMPS-large-scale atomic/molecular massively parallel simulator*. s.l. : Sandia National Laboratories, 2007.
27. **Hu, X. Q., Hu, H., & Yang, W. T.** *QM4D: An integrated and versatile quantum mechanical/molecular mechanical simulation package.*
28. *All-atom empirical potential for molecular modeling and dynamics studies of proteins.* **MacKerell Jr, A. D., Bashford, D., Bellott, M. L. D. R., Dunbrack Jr, R. L., Evanseck, J. D., Field, M. J., ... & Joseph-McCarthy, D.** 1998, The journal of physical chemistry B, Vol. 102, pp. 3586-3616.
29. **http://www.charmm-gui.org. [Online]**